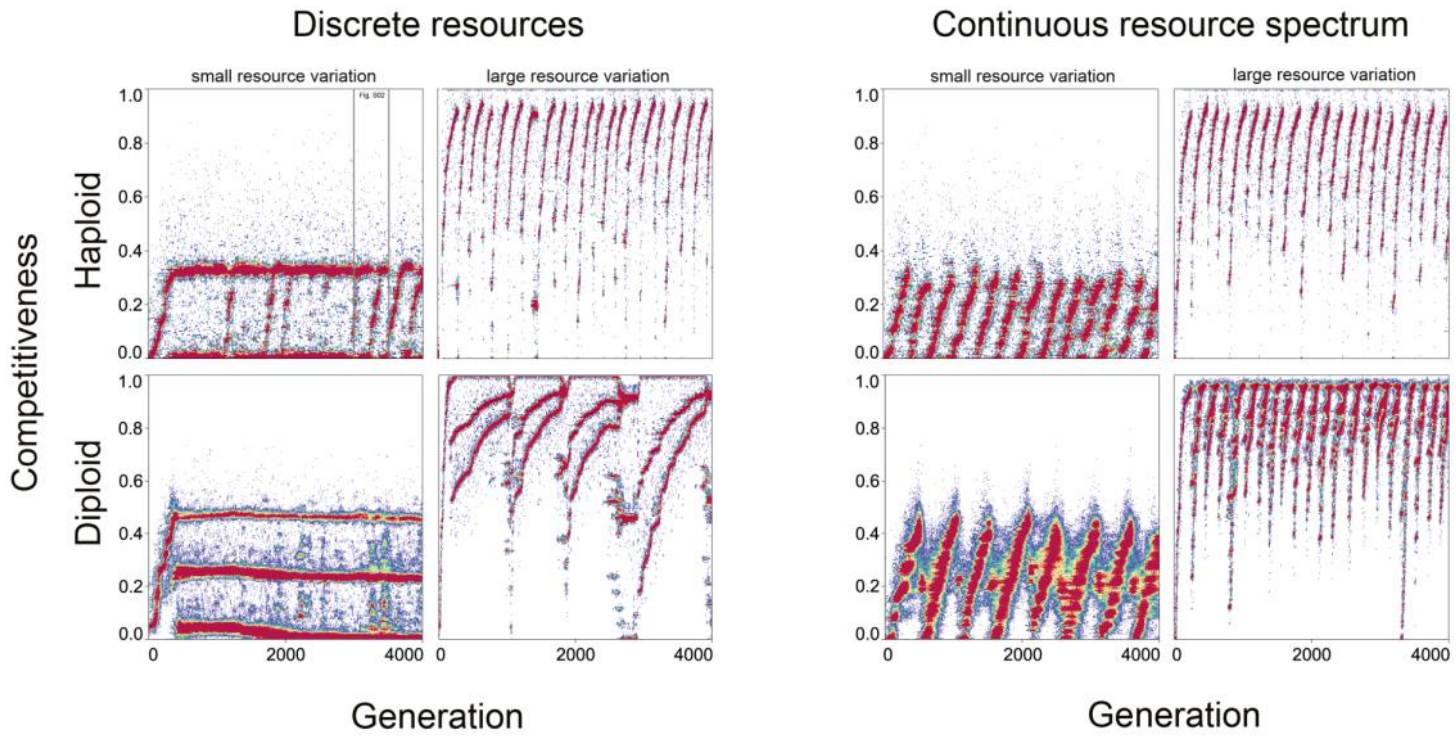

Supplementary Figure 1: Effects of resource distribution, degree of resource variation and the genetic system on the evolutionary dynamics of competitiveness. The two upper left panels (two resources, haploid inheritance) reproduce Fig. 1 in the main text. When resource quality is drawn from a uniform distribution on the interval $[1-\Delta,1+\Delta]$ (two upper right panels), the dynamics is very similar to the discrete case in case of large resource variation ($\Delta = 0.8$), while polymorphism in the discrete case is now replaced by competitive cycles of small amplitude in case of small resource variation ($\Delta = 0.2$). In case of a continuous resource distribution, diploid inheritance leads to a very similar dynamics as haploid inheritance (two lower right panels). In case of discrete resources, diploid inheritance (two lower left panels) leads to polymorphism in case of small resource variation and to competitive cycles in case of large variation. In comparison to the haploid case (two upper left panels), there are now three coexisting genotypes when $\Delta = 0.2$ and polymorphism persists even during competitive cycles when $\Delta = 0.8$.

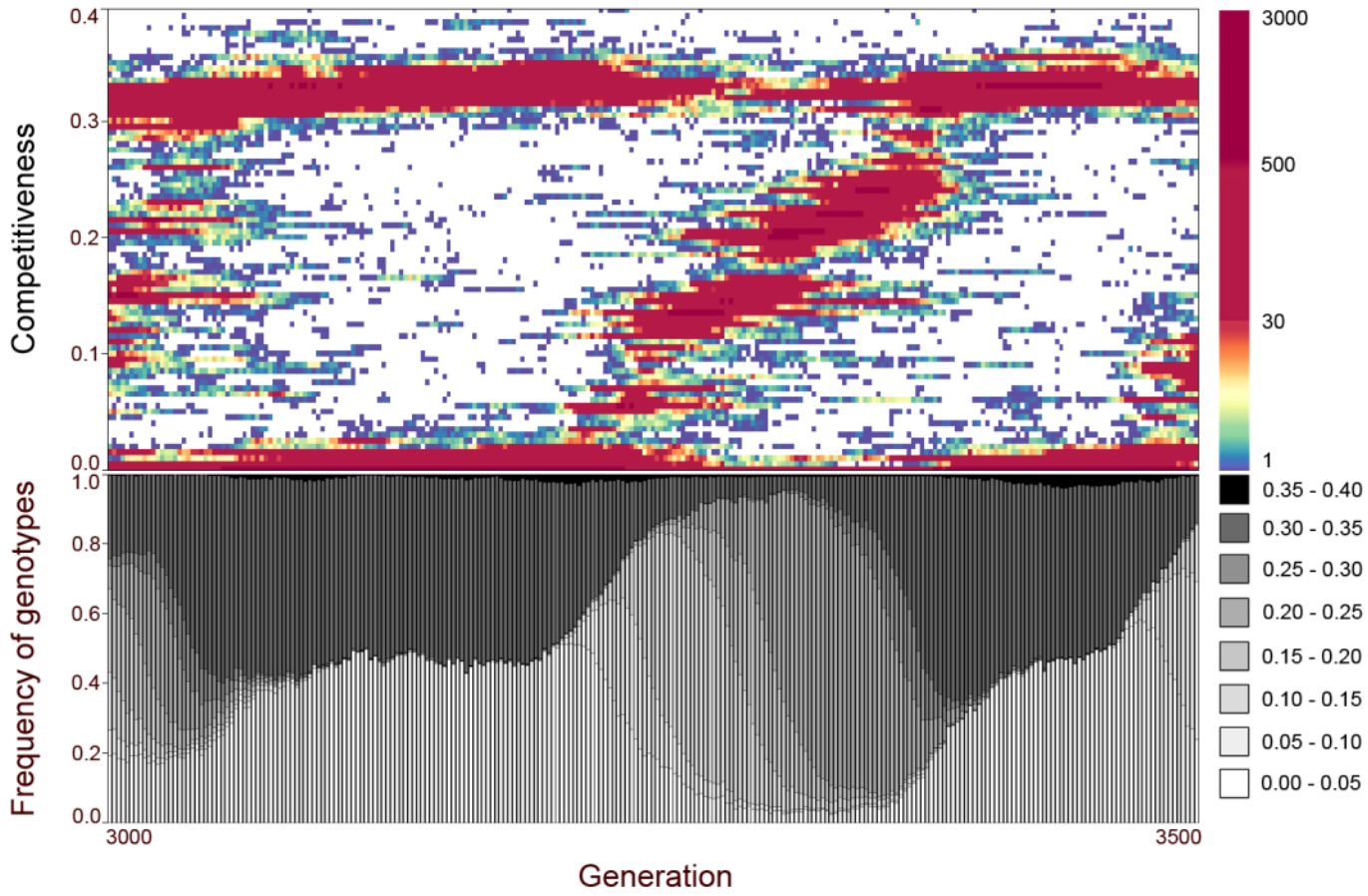

Supplementary Figure 2: A single competitive cycle in a situation where otherwise a low-competitive and an intermediate-competitive genotype coexist in an equilibrium-like situation. The period between generations 3,000 and 3,500 in the simulation shown in the upper left panel of Supplementary Fig. 1(two resources, $\Delta = 0.2$, haploid inheritance), where the standard situation of a stable polymorphism is interrupted by a competitive cycle. The lower panel indicates the corresponding change in the frequency distribution of eight classes of competitiveness genotypes over time during the cycle event. A cycle like this is typically preceded by an increase of the frequency of low-competitive genotypes beyond the frequency of low-quality resources (here 50%).

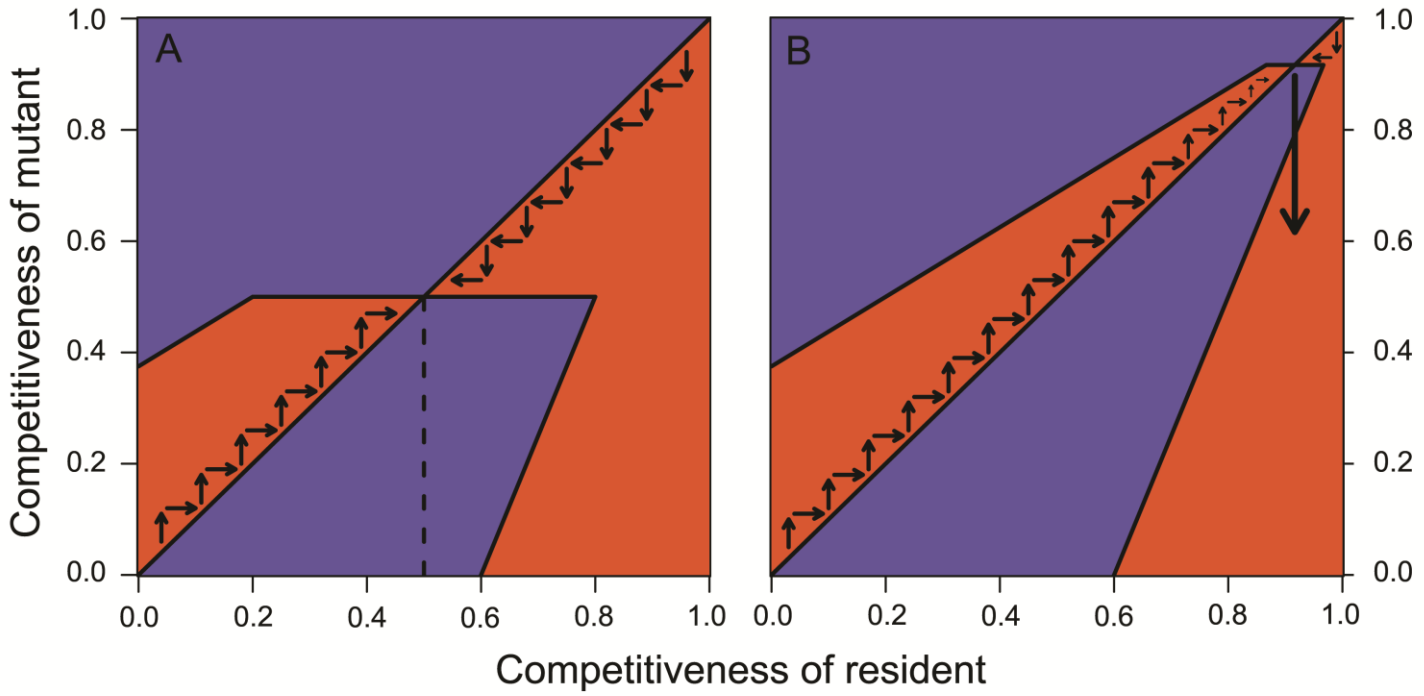

Supplementary Figure 3: Pairwise invasibility plots. In the analytical model, the fitness of a rare mutant with competitiveness c in a resident population with competitiveness $\hat{c}$ is given by $w(c,\hat{c}) = (1-c)\cdot(R_m + \frac{\Delta}{s}(c-\hat{c}))$ if $|c-\hat{c}| < s$, $w(c,\hat{c}) = (1-c)\cdot(R_m + \Delta)$ if $c \geq \hat{c}+s$ and $w(c,\hat{c}) = (1-c)\cdot(R_m - \Delta)$ if $c \leq \hat{c}-s$. Orange regions correspond to situations where mutants have a higher fitness than residents. Mutant strategies are thus able to successfully invade the population (illustrated by vertical arrows) and will eventually replace the resident (illustrated by horizontal arrows). Blue regions correspond to situations where mutants cannot invade. In both cases, repeated gene substitution events shift the population towards an evolutionarily stable level of competitiveness $c^* = 1 - R_m\, s/\Delta$. In (A) $c^* = 0.5$ is globally evolutionarily stable (indicated by the dashed line), whereas in (B) $c^* = 0.92$ is only locally stable, since any larger mutation in the downward direction (indicated by the large vertical arrow that points into the orange region) has a higher fitness and can invade. Parameter values: $R_m = 1$, $\Delta = 0.6$ and $s = 0.3$ in (A), $s = 0.05$ in (B).

The PIPs shown here reflect our assumption that the stochastic error term ε is uniformly distributed over the interval $[-s,+s]$. As a consequence, invasion fitness $w(c,\hat{c})$ is of a particularly simple form, and the border lines between orange and blue regions are piecewise linear. In case of a different distribution of ε (e.g. a normal distribution), the regions are bounded by smooth curves. Qualitatively, however, the PIPs look very similar, and a change in the standard deviation of ε has a similar effect as shown here.

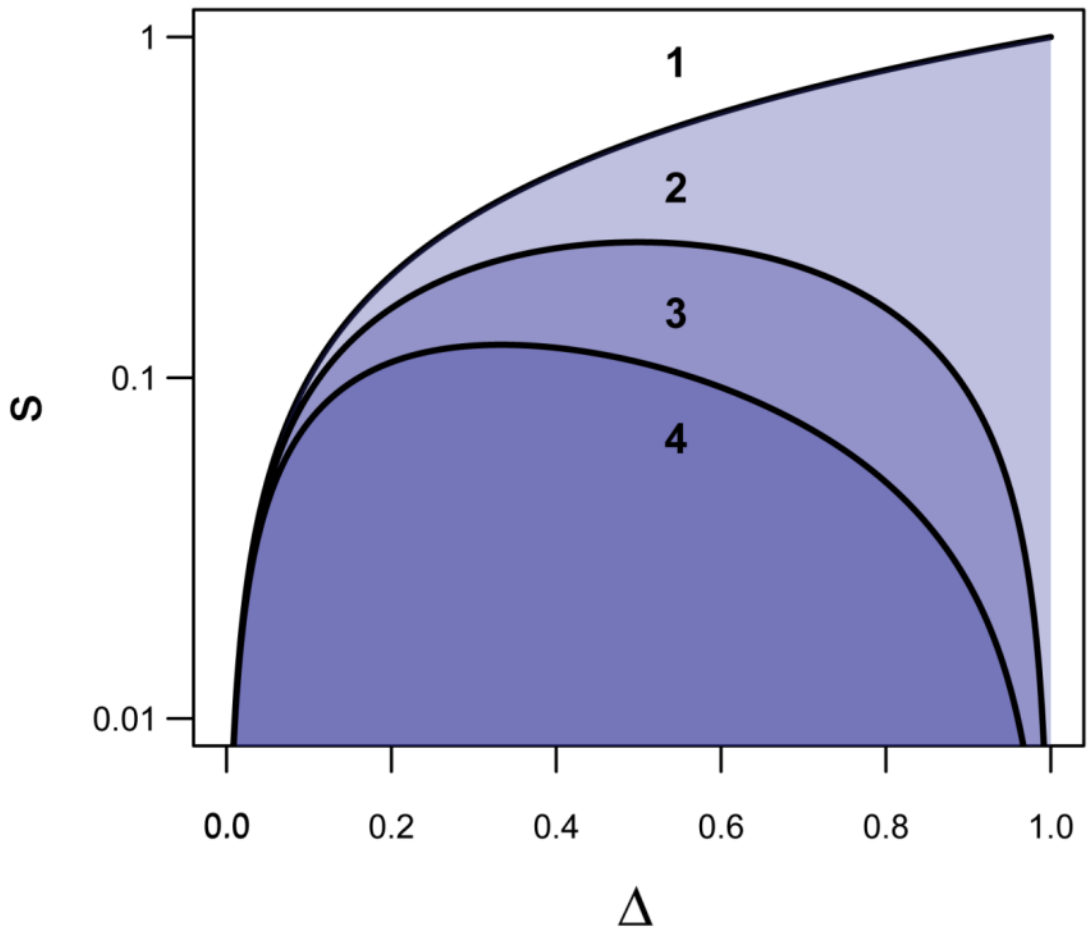

Supplementary Figure 4: Parameter regimes of the four different evolutionary outcomes in the analytical model. For a fixed value of R_m (here $R_m = 1$), the evolutionary dynamics depends on the relationship between s (quantifying the effect of stochasticity on competitive success) and Δ (quantifying the variation in resource quality). In region 1 ($s > \Delta$), competitiveness converges to $c^* = 0$. In the other three regions ($s < \Delta$), $c^* = 1 - \frac{s}{\Delta}$ is an evolutionary attractor. In region 2 ($\Delta(1-\Delta) < s < \Delta$), c^* is globally stable. In regions 3 and 4 ($s < \Delta(1-\Delta)$), c^* can be invaded by mutants with low competitiveness. In region 3 ($s > \Delta(1-\Delta)/(1+\Delta)^2$) such an invasion event typically results in the establishment of a dimorphism, that is, the coexistence of low- and a high-competitiveness genotype. In region 4 ($s < \Delta(1-\Delta)/(1+\Delta)^2$), this dimorphism becomes destabilized as well and the system exhibits perpetual evolutionary cycles. The simulations in Supplementary Fig. 5 illustrate the evolutionary dynamics in regions 2, 3, and 4 (for $\Delta = 0.6$).

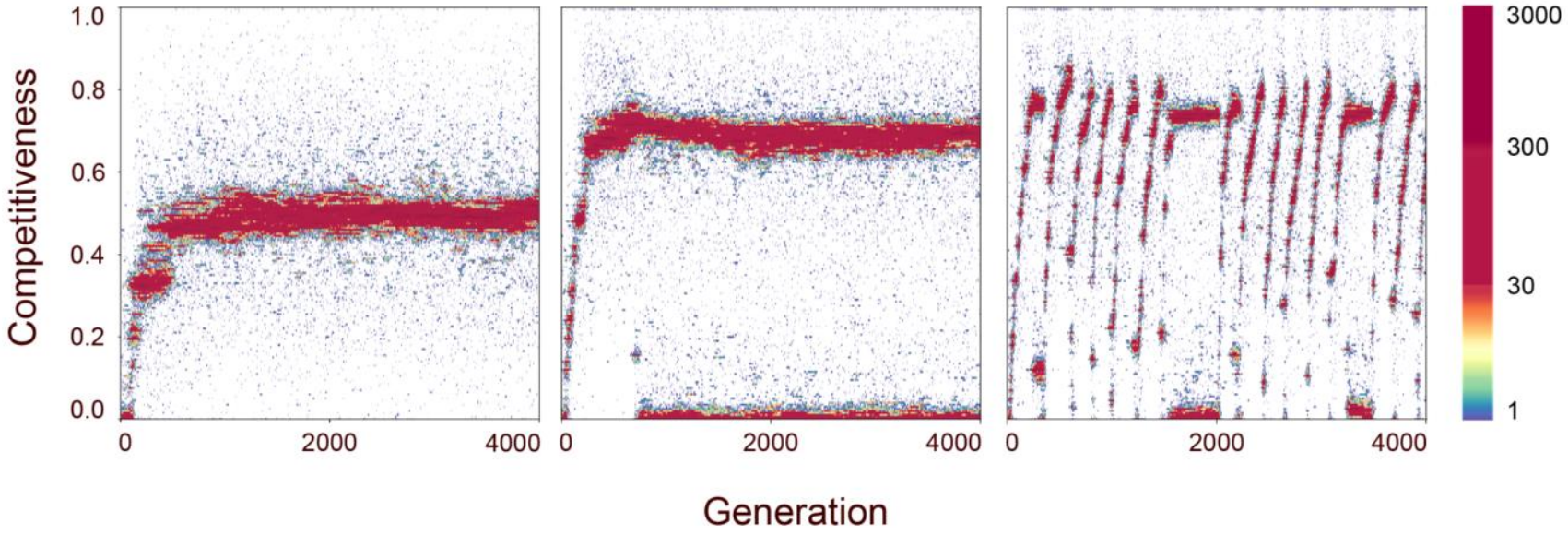

Supplementary Figure 5: Simulations illustrating the evolutionary dynamics in three parameter regimes. Three representative simulations show (for $R_m = 1$ and $\Delta = 0.6$) how the evolutionary outcome changes with a change in the parameter s: For $s = 0.3$ (left panel; region 2 in Supplementary Fig. 4), competitiveness converges to the global attractor $c^* = 1 - \frac{s}{\Delta} = 0.5$. For $s = 0.15$ (middle panel; region 3 in Supplementary Fig. 4), the population first converges to $c^* = 1 - \frac{s}{\Delta} = 0.75$ but subsequently ends up in a dimorphic situation where genotype $c_h^* = 1 - \sqrt{R_{low}\, s/\Delta} = 1 - \sqrt{0.1} = 0.684$ coexists with $c = 0$. For $s = 0.05$ (right panel; region 4 in Supplementary Fig. 4), the population exhibits cycles in competitiveness. To make the simulations comparable to the analytical model, the stochastic error term determining realized competitiveness $c_r = c + \varepsilon$ was drawn from a uniform distribution on the interval $[-s, +s]$. In all other simulations, ε was drawn from a normal distribution with mean zero and standard deviation σ_ε.

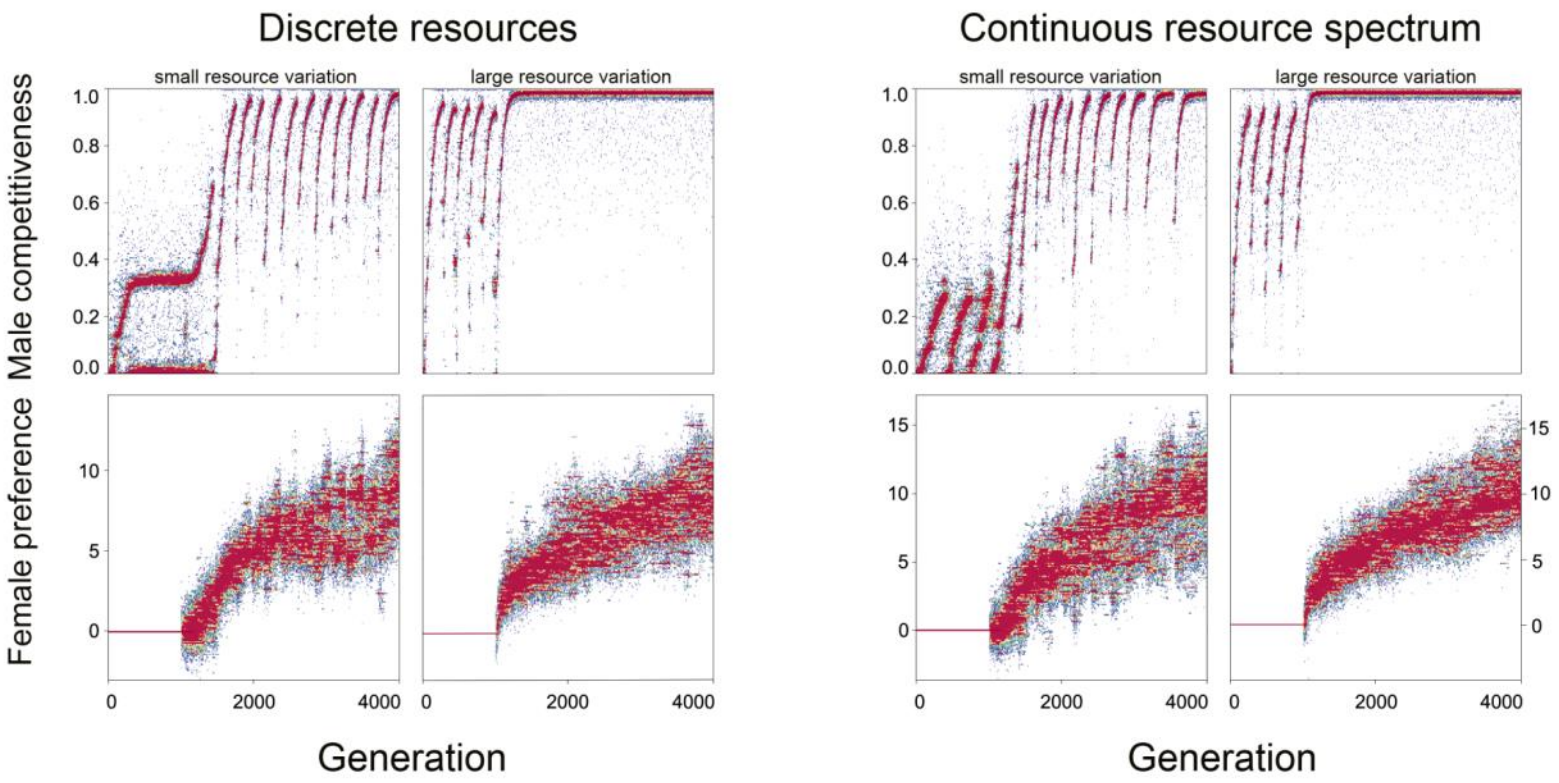

Supplementary Figure 6: Effects of resource distribution and degree of resource variation on the joint evolution of male competitiveness and female preferences. Representative simulations for haploid inheritance and female preferences based on resource quality. Females mated randomly in the first 1000 generations, and female preferences could evolve thereafter. The four left panels reproduce Fig. 2 in the main text; the four right panels show corresponding simulations for the case of a continuous distribution of resource qualities. Also in case of a continuous distribution of resource qualities females evolve preferences for males with high-quality resources. Again, this fuels the evolution in males towards higher levels of competitiveness, resulting in evolutionary cycles ($\Delta = 0.2$) or convergence towards maximal levels of competitiveness ($\Delta = 0.8$).

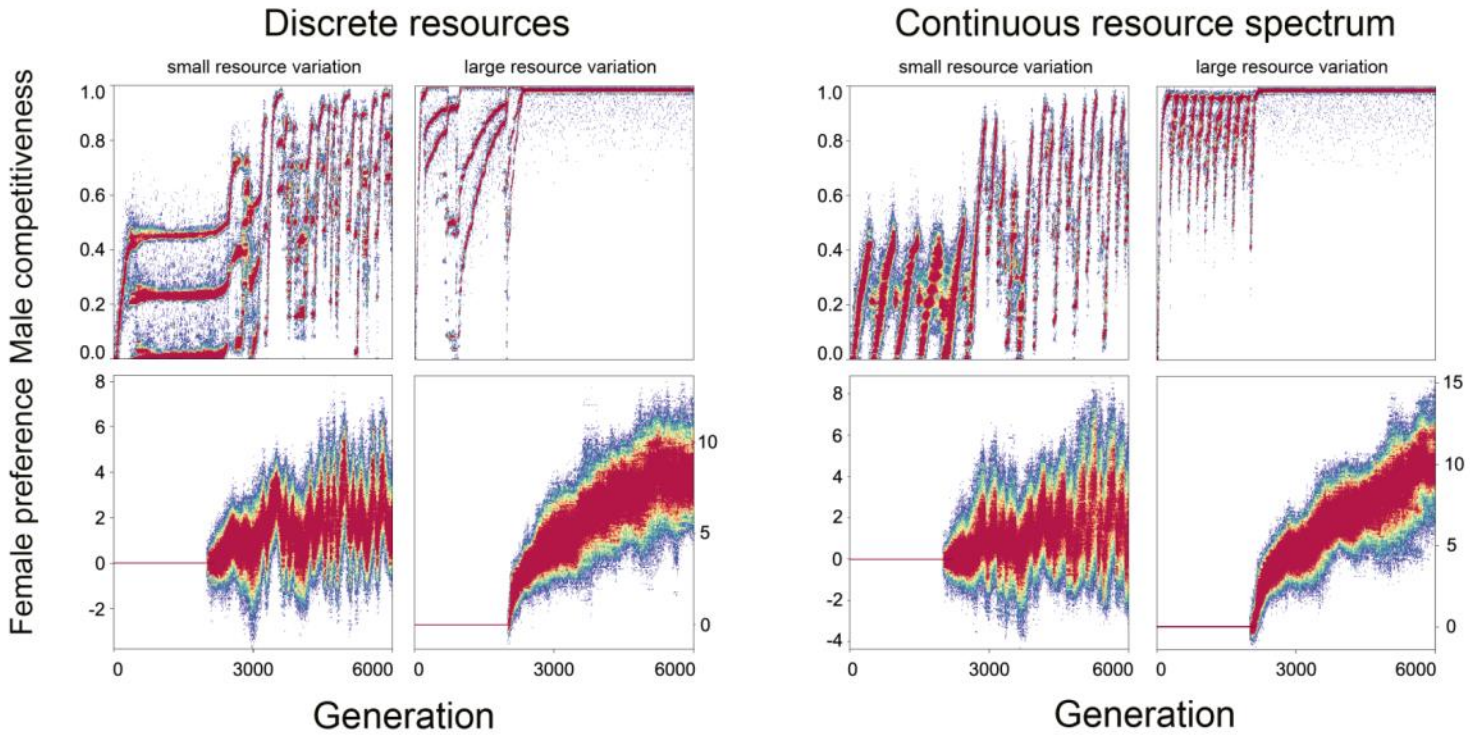

Supplementary Figure 7: Joint evolution of male competitiveness and female preferences in case of diploid inheritance. Representative simulations for the same settings as in Supplementary Fig. 6, but now for diploid inheritance and on a slightly different time scale. Again, female preferences tend to evolve to positive values (a strong preference for high-quality resources). As a consequence, stable polymorphism in competitiveness or small-amplitude cycles in competitiveness give way to large-amplitude cycles, while large-amplitude cycles give way to the fixation of the genotype with highest competitiveness. However, in case of small variation in resource quality, there are periods of time (more closely studied in Supplementary Figs 9 and 10) where a substantial fraction of females has negative *p*-values and hence prefers non-competitive males.

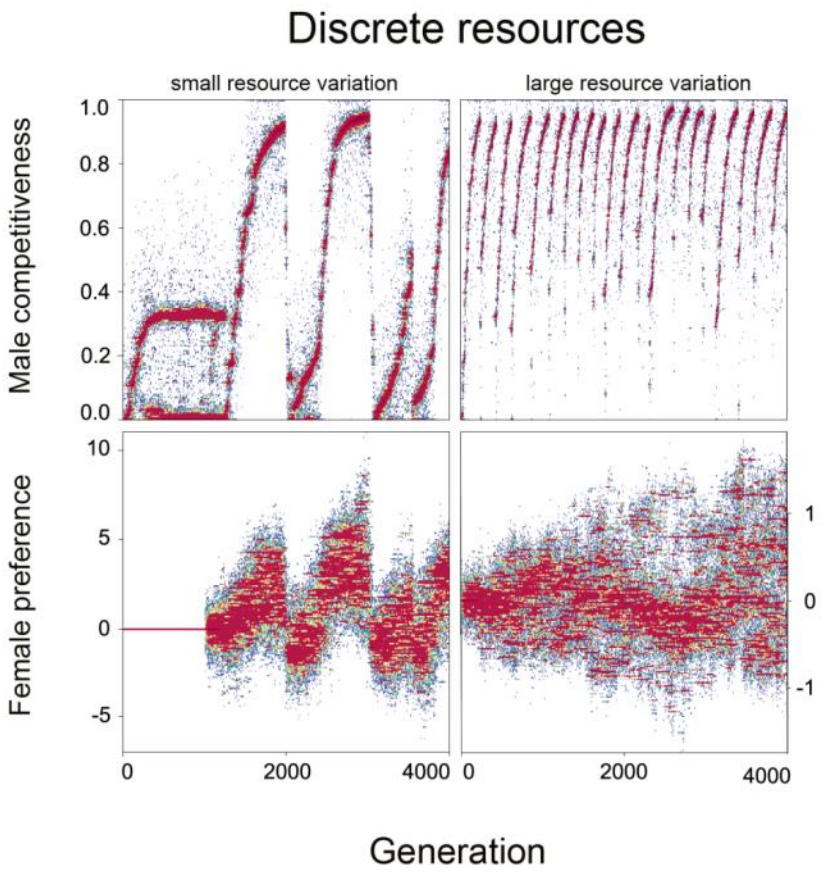

Supplementary Figure 8: Joint evolution of male competitiveness and female preferences when female preferences are based on male competitiveness. Representative simulations for the same situation as in the four left panels in Supplementary Fig. 6 (two resource qualities, haploid inheritance). However, female preferences are not based on resource quality, but on male competitiveness. As before (in the haploid scenarios), females have the tendency to evolve a preference for males of high competitiveness. However, this tendency is less pronounced than in Supplementary Fig. 6, where preferences were based on resource quality. Moreover, in case of small variation in resource quality (left plots), there are periods of time where a fraction of the female population has a negative *p*-value and hence prefers non-competitive males. These periods correspond to periods where male competitiveness drops from very high to very low levels, initiating a new cycle of male competitiveness. When the variation in resource quality is large (right plots), the dynamics of males and females seem largely decoupled, presumably because females cannot adapt to the fast cycles in competitiveness in males. Instead females evolve a broad spectrum of preferences ranging from very negative to very positive *p*-values.

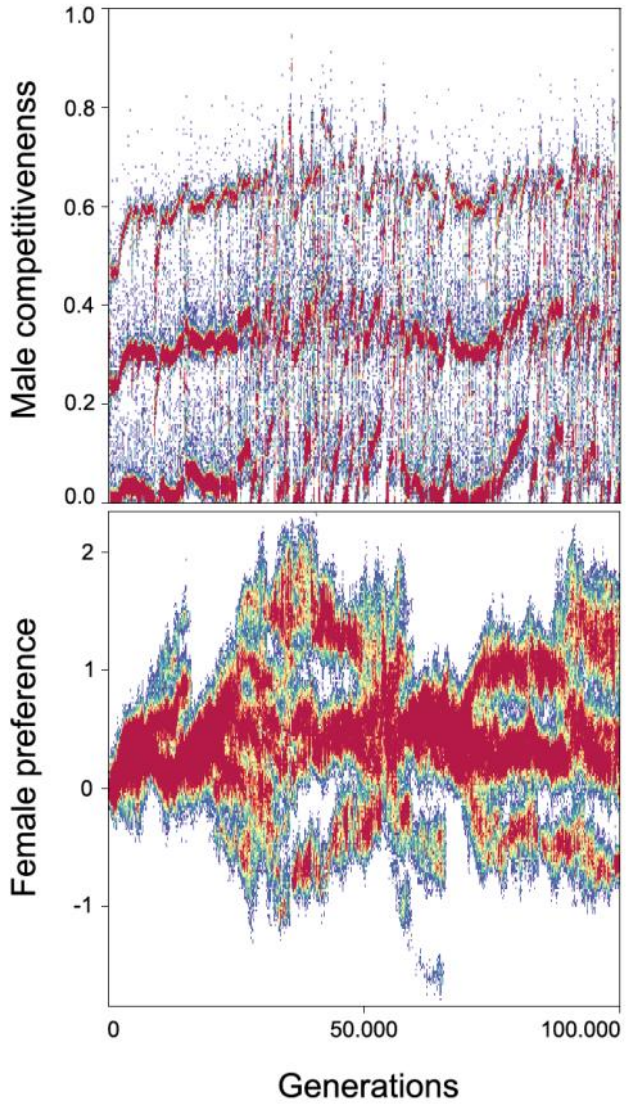

Supplementary Figure 9: Long-term evolution of male competitiveness and female preferences in case of diploid inheritance. The same simulation as in the two left panels of Supplementary Fig. 7 (two resources, $\Delta = 0.2$), but now on a much longer time scale. It becomes evident that the initial increase in female preferences gives way to evolutionary branching and the subsequent coexistence of three different female genotypes: a cluster of (homozygous) genotypes with strong preference for competitive males, a cluster of (homozygous) genotypes with a pronounced preference for non-competitive males; and an intermediate cluster of (heterozygous) genotypes with a weak preference for competitive males. This pattern of preferences induces the coexistence of three types of males with high, intermediate and low competitiveness, respectively.

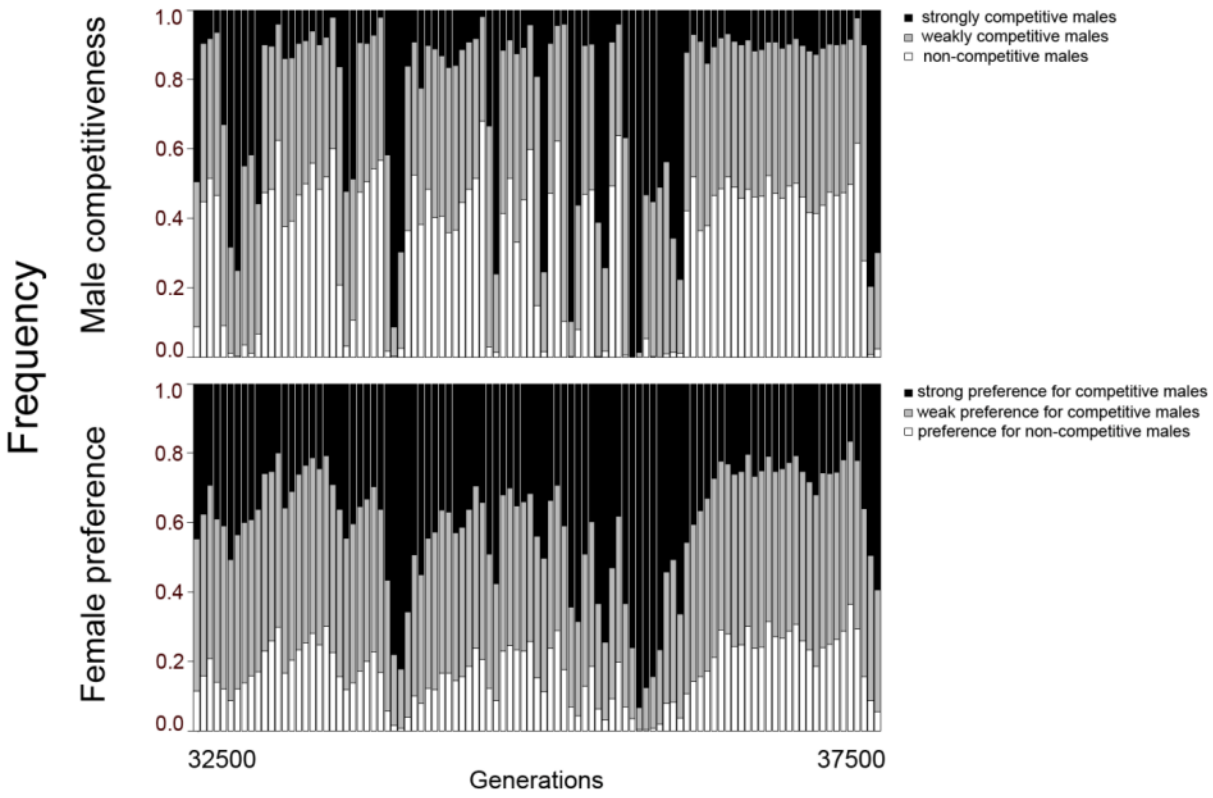

Supplementary Figure 10: A more detailed picture of the time between generations 32,500 and 37,500 in the simulation shown in Supplementary Fig. 9. Each bar represents a time period of 50 generations and shows the frequency distribution of three classes of genotypes. Males (upper panel) are categorized into non-competitive ($0 \le c \le 0.25$), weakly competitive ($0.25 < c \le 0.50$), and strongly competitive ($c > 0.50$). Females (lower panel) are categorized according to their preference: strong preference for high-quality resources ($p > 1.0$), weak preference for high-quality resources ($0 \le p \le 1.0$), and preference for low-quality resources ($p < 0$).The figure illustrates that, on a finer time scale, the dynamics of competitiveness is more complex than Supplementary Fig. 9 suggests.